

General Disclaimer

One or more of the Following Statements may affect this Document

- This document has been reproduced from the best copy furnished by the organizational source. It is being released in the interest of making available as much information as possible.
- This document may contain data, which exceeds the sheet parameters. It was furnished in this condition by the organizational source and is the best copy available.
- This document may contain tone-on-tone or color graphs, charts and/or pictures, which have been reproduced in black and white.
- This document is paginated as submitted by the original source.
- Portions of this document are not fully legible due to the historical nature of some of the material. However, it is the best reproduction available from the original submission.

NAMRL-i220

NASA CR-

147436

NUCLEAR EMULSION MEASUREMENTS OF THE ASTRONAUTS'
RADIATION EXPOSURES ON SKYLAB MISSIONS 2, 3 AND 4.

Hermann J. Schaefer and Jeremiah J. Sullivan

NASA Order No. T-43310G

(NASA-CF-147436) NUCLEAR EMULSION
MEASUREMENTS OF THE ASTRONAUTS' RADIATION
EXPOSURES ON SKYLAB MISSIONS 2, 3, AND 4
(Naval Aerospace Medical Research Lab.)
17 p HC \$3.50

N76-16746

Unclas
13393

CSCI 06R G3/52



NAVAL AEROSPACE MEDICAL RESEARCH LABORATORY

10 December 1975



Prepared for the
NATIONAL AERONAUTICS
AND
SPACE ADMINISTRATION

This document has been
approved for public
release and sale; its
distribution is unlimited.

SUMMARY PAGE

THE PROBLEM

Passive dosimeter packs carried by the astronauts on their wrists contained, among other sensors, nuclear emulsions for recording the radiation exposure on the Skylab missions. Trapped protons encountered in numerous passes through the South Atlantic anomaly were expected to furnish by far the largest part of the mission doses. Because of the long mission times, difficulties in a quantitative track and grain count analysis of the proton energy spectrum were anticipated from latent image fading and track crowding.

FINDINGS

Only the G.5 emulsions flown on the 28-day mission Skylab 2 allowed a quantitative track and grain count at least for a major portion of the spectrum. By comparing the grain count/range functions for different proton tracks ending in the emulsion, the influence of track fading on grain density was determined. Applying these data to the grain count scores, an upper and lower limit energy spectrum was established which defined the margin of error due to fading. Track crowding substantially impaired the identification of tracks with low grain densities. The deficient data for the high-energy section of the spectrum were corrected by assuming that the spectral configuration in the poorly defined region was identical with the one observed on an earlier manned mission on which track crowding had posed no problems. Fading did not impair the proton ender count in K.2 emulsions. The energy spectrum, therefore, was accurately defined for the low-energy section down to zero energy. The dose contribution from tissue disintegration stars was established from the integral star prong spectrum using conventional methods. The prong spectrum also was used for a semi-quantitative assessment of the neutron dose. The three components: protons, tissue disintegration stars, and neutrons were found to account for a mission dose equivalent of 2,490 millirems. A directional analysis of the proton ender population in a K.2 emulsion from a pack kept stationary in a film vault drawer on Skylab 2 revealed a highly structured distribution demonstrating the strong dependence of the fluence of low-energy protons on the local shield geometry. For Skylab 3 and 4, data acquisition was limited to proton ender counts in K.2 emulsions.

The findings indicate that already for Skylab 2 and all the more for Skylab 3 and 4, exposure levels exceeded the range within which the emulsion method can furnish accurate information. However, the measurements demonstrate at the same time how, with special procedures, semi-quantitative data can still be salvaged from emulsions flown on such missions. Such procedures would seem especially useful for coping with unexpected overexposures to protons in space as they would result from solar flares.

INTRODUCTION

As on all manned space missions throughout the Mercury, Gemini and Apollo programs, the radiation exposure of the Skylab astronauts was measured with personnel dosimeters. A small casing carried on the wrist contained nuclear and ordinary film badge emulsions, plastic foils for track etching, neutron activation foils and TLD chips. The following report deals exclusively with the nuclear emulsion findings.

The long mission times of the Skylab flights were expected to aggravate two particular problems in the quantitative evaluation of the mission doses, problems that had been only of minor significance on earlier missions: latent image fading and track crowding. For a Skylab-type orbit, the largest share of the mission dose is contributed by trapped protons encountered in numerous passes through the South Atlantic anomaly. The energy dissipation of the individual proton in tissue depends on its Linear Energy Transfer (LET) which in turn is determined from the grain density of the particle track in emulsion. Latent image fading decreases the grain density progressively with increasing time between exposure and development. As a consequence, tracks imprinted early during the mission show, for the same LET, a lower grain density than tracks imprinted later. Since there is no way of determining ages of individual tracks, the corresponding degree of fading remains undetermined and cannot be corrected for. Fortunately, there is one important exception: the influence of fading on the grain density of proton tracks ending within the emulsion (so-called enders) can be exactly determined. This allows a general appraisal of the fading effect on the contributions from all tracks to the exposure.

Track crowding, i.e., the overloading of the microscopic visual field with track segments, impedes accurate grain counting and can mask completely track segments of low grain density. Severe crowding as it occurred in the G.5 emulsions of Skylab missions 3 and 4 goes even further by interfering with proper image formation in transmitted light and can block track counting completely. Microtoming such emulsions down to thicknesses of 5 to 7 microns is a limited remedy, but creates new problems because such thin layers contain only very few long track segments. On Skylab missions 3 and 4, track crowding essentially limited quantitative work to proton ender counts in the less sensitive K.2 emulsions. By linking these ender counts to Skylab 2 the corresponding total doses from protons could still be inferred to satisfactorily.

LATENT IMAGE FADING

Latent image fading in photographic emulsion depends on three environmental factors, relative humidity, oxygen concentration and temperature. It decreases as these three factors decrease. While ways and means exist to keep emulsion at low temperature in an oxygen-free atmosphere, keeping it for longer periods at zero or very low humidity deteriorates the structure of the gelatin matrix rendering the emulsion layer brittle and leading to cracks and aticulation. Therefore, a compromise has to be found by selecting a moderately low humidity and accepting a certain degree of fading.

How fading affects the determination of particle energy from the grain count will be discussed now directly with the scanning scores of a G.5 emulsion from Skylab 2. Long proton enders were identified in the emulsion and their grain density as a function of residual range determined. The individual curves were found to differ for different tracks reflecting the different ages of the tracks and corresponding degrees of fading. Two extremes assumed to represent the lowest and highest degree of fading were selected. Figure 1 shows grain count as a function of residual range in emulsion for the two tracks. Converting range to kinetic energy, we obtain the

curves in Figure 2 showing grain count as a function of energy. For a quantitative assessment of the influence of fading on the determination of dose, energy has to be converted to LET. Table 1 shows the pertinent relationship for selected grain densities in Figure 2. It is seen by inspection that the range of uncertainty in terms of LET due to fading strongly depends on the energy or LET of the particle. It is small at high energy, i.e., low LET, yet large at low energy, i.e., high LET.

In view of the fact that the exposure to protons on the Skylab missions was evenly distributed in time with passes through the anomaly occurring on an identical daily schedule, one could think of drawing the mean curve between the two extremes in Figure 2 and using the corresponding energy/grain count function for evaluating all track segments. While this approach certainly would furnish the closest possible approximation to the true energy spectrum of the proton exposure, one might prefer, in radiation safety monitoring, an alternate approach that would furnish a conservatively high value for the dose. This more cautious method would select the grain count/energy function for the most faded ender, i.e., the lower curve in Figure 2, and apply it to the grain count scores of all track segments. In doing so, one underrates the energy of all track segments of lesser fading, i.e., one overrates their LET and contribution to the mission dose.

ENERGY SPECTRUM OF PROTON EXPOSURE ON SKYLAB 2

Establishing the energy spectrum for a population of proton tracks by track and grain count analysis is an extremely time-consuming task. Furthermore, it seems a reasonable assumption that the configuration of the spectrum within the vehicle after the incident radiation has travelled through considerable shielding will not be greatly different any more at different locations. It seems acceptable, then, to limit the track and grain count analysis to one emulsion sheet taken from the pack of one crew member and to infer to the doses for the other two crew members from the respective ender counts in emulsions of their dosimeter packs.

A 50 micron Ilford G.5 emulsion developed moderately strong in Amidol from Pack 3A, carried by the pilot, was selected for full analysis. With a 90x oil immersion objective and 10x eye pieces, squares of 70 x 70 microns corresponding to elementary volumes of 50 x 70 x 70 microns of unprocessed emulsion were scanned. All tracks of sufficiently high grain density to be recognized were measured with regard to their three-dimensional lengths and their grain counts. A total of 996 track segments was analyzed.

In the actual scanning, grain densities have been counted up to about 200 grains/100 microns Em. However, all track segments with counts $> 160\text{gr}/100\ \mu\text{Em}$ were pooled in one class for data evaluation and re-distributed computationally so that a smooth terminal section of the energy spectrum was obtained. The same class also contained all segments representing so-called black tracks, i.e., tracks of such a high grain density that the grains coalesce to a solid silver ribbon.

In the following data presentation, the concept of the equivalent uni-directional fluence is used. That means particle fluence is expressed in terms of a parallel beam of protons which would produce, in the scanned emulsion volume, a combined total track length equal to the one actually observed. Table II presents the results of the grain count analysis. Columns 1 and 2 show the class limits for grain density. The corresponding class limits for energy as they follow from the lower curve in Figure 2 are shown in Columns 3 and 4 and for the upper curve in Columns 5 and 6. Column 7 shows the raw scores of the combined lengths of track

segments in each class with observed values expressed in terms of equivalent unidirectional fluence as explained above. Finally, Column 8 shows the cumulative sum of the values in Column 7. That means, Column 8 presents values of integral fluence. Two different integral energy spectra are defined by Column 8 depending upon whether one uses the energy classes defined in Columns 3 and 4, or 5 and 6. The two spectra are shown in Figure 3. In the same way as in Figure 2, the shaded area between the two curves delineates the corridor within which the curve of the true energy spectrum must run. It was mentioned before that in radiation safety monitoring a conservatively high estimate of radiation exposure might be preferable. In line with this suggestion, one would have to select the upper contour in Figure 3 for the evaluation of LET distribution and dose.

A cautious approach should also be followed in correcting the second systematic error in the raw scores of the grain count mentioned above. We mean the missing of tracks in the scanning process due to crowding. In a microscopic visual field overloaded with grey and black tracks, the scanner misses tracks with low and very low grain densities. The critical grain density at which the number of missed tracks assumes sizeable proportions is not sharply defined since it depends strongly on the slant angle at which a particular track crosses the plane of sharp focus. Because of this dependence, the error increases gradually as grain density decreases. We strongly suspect that the saturation of the curves in Figure 3 toward higher energies reflect the error due to the crowding effect and is not truly representative of the spectrum.

We have tried to make a quantitative assessment of the error due to missed tracks by comparing the Skylab 2 spectrum with the one observed on the first lunar landing mission, Apollo 11. On the latter flight, the proton fluence was only about one tenth of the one on Skylab 2. Therefore, no crowding problems existed and the grain count scores reliably defined the spectrum up to very high energies. Characteristically, the two spectra show, in the energy region below 50 Mev, very nearly the same configuration if fluences are normalized. It appears acceptable, then, to assume that the similarity of the two spectra extends upwards into the energy region above 50 Mev. The uniform continuation of the upper curve in Figure 3 beyond 50 Mev is based on this assumption. It represents the integral energy spectrum of the proton fluence on Apollo 11 normalized to the much larger fluence on Skylab 2 at 50 Mev. The corrected upper contour in Figure 3, then, represents a conservatively high approximation to the true energy spectrum of the proton fluence on Skylab 2.

Looked at from a wider scope, Figure 3 describes well the two basic limitations of the nuclear emulsion technique for measuring proton energy spectra in space in general. Both limitations ultimately result from the long duration of the mission in as much as fading as well as track crowding become more pronounced as exposure time increases. Because fading had been anticipated as a problem on the Skylab missions from the beginning, appropriate measures had been taken in preparing and sealing the emulsion packs. Therefore, the corridor of the fading error in Figure 3 based on the Skylab 2 recordings can be considered as typical for the optimum that can be accomplished. However, one should remain aware of the fact that the terminal section of the spectrum from about 5 Mev down to zero not shown in Figure 3 always can be reliably established from the proton ender count which is not subjected at all to any error from fading or crowding. Therefore, as long as normal conditions prevail, i.e., no solar activity of major proportions develops, the ender count will furnish a satisfactory semi-quantitative measure of proton exposure even for missions of substantially longer duration than Skylab 2. In support of this conclusion, we submit below the proton ender count for the 56 and 85-day Skylab missions 3 and 4.

It should be pointed out that the energy spectrum presented in Figure 3 has been recorded with nuclear emulsion close to the body of the astronaut. To what extent it can be considered representative for tissue is a complex problem. It is obvious that an infinitely thin layer of emulsion in contact with the skin records the same fluence and spectrum which would enter the body of the astronaut without the emulsion present. For an emulsion layer of finite thickness this proposition still holds for protons that lose only a negligible part of their total energy in the emulsion layer. However, as one proceeds to particles of lower energies, the fractional energy loss in emulsion can no longer be neglected. That means that the low-energy section of the spectrum as recorded in emulsion is not representative any more for the spectrum as it would prevail at the body surface not covered with emulsion. Fortunately the low-energy section can be determined, without any grain counting, from the frequency of tracks that enter from the outside yet end within the emulsion layer. It is easily seen that the number of such enders per unit volume of emulsion and tissue directly reflect, for the same incident spectrum, the respective Stopping Powers of the two media. The observed ender count in emulsion therefore, can be converted directly to the corresponding count in tissue simply by applying the Stopping Power ratio as a scaling factor. At the same time, the ender count is not subjected to any error due to fading because even the most faded ender still stands out conspicuously, especially in the lower background of the less sensitive K.2 emulsion. The ender count, therefore, accurately defines the anchor point of the spectrum at zero energy. In an earlier publication (1), the utilization of the ender count in combination with the spectrum in Figure 3 for establishing the tissue equivalent LET distribution and dose on Skylab 2 has been described in detail. As pointed out there, the combined method leads to a mission dose from protons of 1140 millirads or 1760 millirems.

By far the largest share of the just quoted dose accrues from trapped protons encountered in numerous passes through the South Atlantic anomaly. However, trapped particles are not the only source of protons. As Freier and Waddington (2) have pointed out, the primary cosmic radiation in space produces, in the local hardware of the vehicle, numerous low-energy secondary protons in nuclear interactions. These reactions are responsible for the star phenomenon in emulsion which will be analyzed in more detail in the next section. At this point it might suffice to mention that 75 percent of the secondary protons result from evaporation stars and are essentially limited to the energy region below 30 Mev. The balance of 25 percent is produced in knock-on stars, furnishing secondaries of higher energies that tend to be collimated in the forward direction. To the extent to which secondaries from nuclear interactions originate in materials other than the emulsion layer itself, they represent a legitimate component of the radiation to be measured. The particular origin of a particle is irrelevant as far as the radiation load of the astronaut is concerned. In order to identify all enders originating in the emulsion, we have traced, in the scanning process, all enders back to their points of origin. If they entered the emulsion from the outside, they were counted. If they originated from stars in the emulsion, they were rejected in the count. Because a certain fraction of the rejected enders originate in the gelatin matrix of the emulsion and therefore represent a tissue-equivalent component, the method, at first sight, appears to underrate the ender frequency that accounts for the tissue dose. However, the loss is fully compensated for because the dose contribution from all secondaries of tissue stars is established separately as described in detail in the next section.

DOSE CONTRIBUTION FROM TISSUE DISINTEGRATION STARS.

A problematic issue of space radiation dosimetry in general is the dose contribution from secondaries released in nuclear collisions in the body tissues themselves. From their characteristic appearance in emulsion these disintegrations are called stars. Since half the volume of

nuclear emulsion is occupied by gelatin, a sizeable fraction of the star population in emulsion originates in tissue equivalent material and therefore is directly indicative of the tissue dose. However, discriminating individual stars originating in the gelatin matrix from those in the silver halide is not possible. Merely two indirect methods exist for separating the two components of the total star population. At best, they furnish semi-quantitative estimates of the tissue dose that would develop in a layer of 100 percent gelatin replacing the emulsion. One method divides the total star frequency into two fractions applying the ratio of the respective cross sections for nuclear interactions of the two component media. The other does essentially the same graphically by evaluating the change of slope of the integral prong number spectrum of the total star population. Both methods have been proposed by Birnbaum and co-workers (3) and have been described in their application to space radiation data in an earlier publication of this laboratory (4).

Applying the second method to the star data from the K.2 emulsions of Skylab 2, we have pooled, in the interest of better statistics, the star counts from all scanned K.2 emulsion sheets. This procedure appears acceptable in view of the fact that stars are produced predominantly by primary particles of high energy, i.e., high penetrating power. Differences due to local variations in shielding for different packs therefore can be assumed to be small. A grand total area of 33 mm^2 of K.2 emulsions of 100 micron thickness has been scanned. Figure 4 shows the integral prong number spectrum of the total star population. The discontinuous change of slope of the spectrum at the abscissa value of 7 is conspicuous. It indicates the onset of the additional star production in the gelatin matrix which, because it contains only light elements, can contribute only stars with a highest prong number of 7 or 8. The fractional star population contained in the shaded area of Figure 4 originates in the gelatin matrix. The corresponding numbers derived from the straight lines of best fit are shown in Table III. Applying to the fractional star population from the gelatin the constants proposed by Davison (5), (3.7 mean number of prongs per star, 14 Mev mean energy per prong, 6.5 mean QF), we obtain a mission dose from tissue disintegration stars of 98 millirads or 591 millirems. The comparatively high mean QF value results from the fact that low-energy alpha particles account for a substantial percentage of the star prong population. Because of the high QF, tissue stars account for a sizeable fraction of the grand total dose equivalent. In view of this fact, the design of methods for direct and more precise measurements of the tissue star dose equivalent appears highly desirable.

Disintegration stars not only produce protons and alpha particles, but also neutrons. However, neutrons do not produce visible prongs in nuclear emulsion. Because of their completely different attenuation mechanism they diffuse out to much greater distances from the star center than do protons and alpha particles. They finally terminate, after several or many elastic collisions, in capture reactions. In hydrogenous material such as tissue, by far the largest share of the total energy of star produced neutrons is dissipated by recoil protons. The energy spectrum of proton recoils centers heavily on the region closely below 1 Mev. Accordingly, the tracks of the recoils in emulsion are quite short. Their identification in emulsions exposed to the heterogeneous radiation field in space therefore is extremely difficult. In fact, the bulk of the population of neutron recoils remains masked by blobs of terminating electrons and other grain configurations from which the short recoil tracks cannot be clearly distinguished. Therefore, the neutron dose shares the fate of the tissue star dose. It can be determined only semi-quantitatively by indirect methods.

In evaporation stars, neutrons are produced with a slightly higher abundance than protons. The assumption of equal abundances for the two components then will provide a safeguard

against exaggeration of the dose contribution from the neutron component. Assuming furthermore, a proton to alpha abundance ratio of 0.41 to 0.18 and using again Davison's (5) model for the average evaporation star, we obtain a mean number of 1.52 neutrons per star. The star count for the gelatin matrix in the K.2 emulsions of Skylab 2 reported in Table III corresponds to a frequency of 1.12×10^5 stars/cc Em. Assuming again a mean energy per neutron of 14 Mev dissipated exclusively in ionization processes of recoils we arrive at an absorbed dose of 38 millirads. Official regulations assign a QF of 10 to fast neutrons, which leads to a mission dose equivalent of 380 millirems.

It seems of interest to compare the neutron dose as it follows from our star count in emulsion with the neutron dose which one can establish theoretically from the galactic neutron spectrum in free space and its transition in the Earth's atmosphere. A number of elaborate theoretical and experimental investigations have been conducted on the latter phenomenon. Attempting to weigh properly somewhat discrepant data communicated by Hess and co-workers (6) and by Armstrong and co-workers (7), we arrive at a galactic neutron radiation level of 520 microrems/hour in the transition maximum within the atmosphere for conditions of solar minimum and high latitudes. Multiplying with a total time in orbit of 672 hours for Skylab 2, we obtain a mission dose equivalent of 350 millirems from galactic neutrons. The actual value must have been markedly smaller because the Skylab vehicle sweeping continuously from latitude 52° North to 52° South spent a considerable fraction of its total time in orbit at low latitudes where the galactic neutron fluence is well below its saturation value at high latitudes. It is seen then that the experimental value of the neutron dose equivalent as it follows from our star count is substantially larger than the theoretical value for the galactic contribution. This seems to indicate that a sizeable portion of the neutron fluence on Skylab 2 originated in star events triggered by trapped protons in the anomaly.

Summarizing the contributions of the three components discussed in the preceding section, we arrive at a total dose equivalent of 2,490 millirems. It should be realized that this value does not include the electron component. The dose contribution from electrons can not be measured with nuclear emulsions, because the heavy background from nuclear particles does not allow a separate densitometric evaluation of the background from electrons. Inspection of G.5 emulsions cut on the microtom to a thickness of 7 microns conveys the general impression that the dose from electrons, though not a sizeable portion, would need to be considered in an accurate assessment of the total mission dose. It is seen then, that the dose equivalent of 2,490 millirems represents a lower limit of the true radiation exposure on Skylab 2. More specifically, it represents the dose from all nuclear particles entering the astronaut's body which can be grain-counted. This means that alpha particles and some "light" HZE particles are included. However, their contribution to the mission dose remains quite small.

PROTON ENDER COUNTS

As mentioned in the preceding part of this report the long duration of Skylab Missions 3 and 4 (56 and 84 days) saturated the G.5 emulsions to such a degree that even a semi-quantitative grain count evaluation was impossible. We have succeeded in cutting G.5 emulsions on the microtom with a special technique. Sections with a thickness of 5 to 7 microns allow excellent microscopic observation and identification of track segments. However, the majority of the track segments in such thin layers are quite short and therefore offer only a small number of grains for the count. Because of the large statistical variations of the grain density along a track, LET and energy carry a substantial error if based only on a small number of counted grains. For this reason, we have decided not to invest the large amount of scanning man-hours

needed for a grain count analysis. Instead, we have concentrated the scanning effort entirely on proton ender counts in the K.2 emulsions flown on Skylab 3 and 4. Table III summarizes the ender counts for three Skylab Missions. It should be emphasized that the ratios of the ender counts do not directly indicate corresponding ratios of the total proton doses. Because enders represent the low energy section of the spectrum their frequencies reflect differences in the local shield distributions more sensitively than do the total proton fluences and the corresponding doses.

The strong dependence of the local ender count on shielding is well demonstrated in measurements of the directional distribution of enders which we conducted for radiation pack 6-A which was kept stationary in drawer F of the film vault on Skylab 2. Figure 5 shows the results of the directional analysis. The highly structured distribution reflects the complex shielding geometry about the pack. So far, no attempt has been made to align the curves in Figure 5 with the shield distribution of the Skylab vehicle. Because of the geometrical factor, effective shield thicknesses differ from nominal thicknesses most strongly for materials in close proximity of the emulsion pack. Therefore, the geometrical position of the pack in the film vault drawer has to be known very accurately and the corresponding shield distribution of the entire vehicle established. It seems questionable whether the very large effort involved in this task is really worthwhile. Even without the distribution in question available, the data in Figure 5 demonstrate well the directional anisotropy of the low-energy proton fluence. With the basic configuration of the complete energy spectrum known, an analysis of the influence of shielding can be conducted in reversed direction much more easily. Taking fractional fluences for small solid angles of incidence from Figure 5, one can reconstruct the corresponding total spectra for these individual directions of incidence and determine the pertinent variations in shield thickness. Computational procedures for the latter task are greatly facilitated if the energy spectrum is converted to the range spectrum.

CONCLUSIONS

It is quite obvious from the data presented in this report that the objective of a quantitative determination of the dose equivalent for the proton exposure with nuclear emulsions has not been fully met on the Skylab missions. However, the attempted measurements are of considerable interest because the long flight time created the first real overexposure to protons on a manned mission. The Skylab emulsions, therefore, can be exploited as a dress rehearsal of what could be salvaged in case of an unexpected overexposure due to a solar flare. Looking at the results from this particular point of view, we draw the following conclusions.

The most important finding certainly is that a proton ender count in K.2 emulsions has been accomplished even for the 85-day Skylab 4 mission without any impairment from fading or crowding. In fact, both factors interfere, even in the K.2's of Skylab 4, so little with the scanning process that we feel an accurate ender count could still have been retrieved for a mission duration of 100 to 120 days. It is beyond the scope of this report to analyze in detail the margin of error within which the full proton spectrum can be extrapolated from the ender count. With ender counts from nuclear emulsions and total mission doses from TLD measurements now available for a large number of orbital and deep-space missions of the Gemini, Apollo and Skylab programs, such extrapolations could be made empirically with acceptable reliability. Admittedly, combined ender and TLD data are not available for mixed exposures to trapped and flare-produced protons. However, flare spectra in general are known to show substantially steeper slopes than spectra of trapped protons. The bulk of the dose from a flare exposure, therefore, centers more heavily on the low energy section of the spectrum. It is seen by

inspection that this would lead to an overestimate of the total dose if the ender/TLD ratio for trapped protons is applied to the ender count of a mixed exposure. Since this introduces a safety margin in the assessment of the mission dose, it appears entirely acceptable in a record of personnel exposure.

REFERENCES

1. Schaefer, H.J., Problems of Component Discrimination in Space Radiation Dosimetry. Rad. and Environm. Biophys., 12: 127-137, 1975.
2. Freier, P.S., and Waddington, C.J., Electrons, Hydrogen Nuclei, and Helium Nuclei Observed in the Primary Cosmic Radiation during 1963. J. Geophys. Res., 70: 5753-5768, 1965.
3. Bimbaum, M., Shapiro, M.M., Stiller, B., and O'Dell, F.W., Shape of Cosmic-Ray Star-Size Distributions in Nuclear Emulsions. Phys. Rev., 86: 86-89, 1952.
4. Schaefer, H.J., Benton, E.V., Henke, R.P., and Sullivan, J.J., Nuclear Track Recordings of the Astronauts' Radiation Exposure on the First Lunar Landing Mission Apollo XI. Rad. Resch., 49: 245-271, 1972.
5. Davison, P.J.N., Radiation Dose Rates at Supersonic Transport Altitudes. M.O.A. Grant PD/34/017. Farnborough, Hampshire, England: Royal Aircraft Establishment, 1967.
6. Hess, W.N., Canfield, E.H., and Lingenfelter, R.E., Cosmic-Ray Neutron Demography. J. Geophys. Res., 66: 665-677, 1961.
7. Armstrong, T.W., Chandler, K.C., and Barish, J., Calculations of Neutron Flux Spectra Induced in the Earth's Atmosphere by Galactic Cosmic Rays. J. Geophys. Res., 78: 2715-2726, 1973.

TABLE I

GRAIN DENSITY, ENERGY
AND LET FOR FRESH AND FADED TRACKS
IN ILFORD G.5 EMULSION

Grain Density, gr/100 microns Em	Kinetic Energy, Mev		Linear Energy Transfer, kev/microns Em	
	Fresh Track	Faded Track	Fresh Track	Faded Track
25	49.20	37.15	3.09	3.85
50	17.38	13.80	6.94	8.21
75	9.840	7.656	10.65	12.83
100	6.383	5.408	14.50	16.26
125	4.305	2.904	19.05	24.60
150	2.735	1.603	25.60	36.80

o

TABLE II

GRAIN COUNT ANALYSIS OF PROTON FLUENCE IN G.5 EMULSION ON SKYLAB 2

Grain Density, gr/100 μ Em		Kinetic Energy, Mev				Equivalent Unidirectional Fluence, Protons/cm ²	
From	To	Fresh Track		Faded Track		Class	Total
		From	To	From	To		
20	30	361	182	268	139	36,000	1,555,200
30	40	182	118	139	93.1	63,500	1,519,200
40	60	118	67.4	93.1	53.2	282,800	1,455,700
60	80	67.4	44.8	53.2	36.2	364,600	1,172,900
80	100	44.8	32.0	36.2	24.1	282,500	808,300
100	120	32.0	22.9	24.1	16.2	160,700	525,800
120	140	22.9	16.5	16.2	10.4	135,900	365,100
140	160	16.5	11.1	10.4	6.0	102,300	229,200
> 160		< 11.1		< 6.0		126,900	126,900

TABLE III

PROTON ENDER FREQUENCIES IN K.2 EMULSIONS FROM CREW PASSIVE DOSIMETERS
ON SKYLAB 2, 3 and 4

Mission	Pack Number	Position	Number of Enders Counted	Ender Frequencies N/mm^2 $200\mu K.2$
Skylab 2 28 Days	1A	CDR	149	308
	2A	SPT	1499	364
	3A	PLT	632	366
Skylab 3 59 Days	1A	CDR	1011	883
	2A	SPT	1415	1189
	3A	PLT	1274	1023
Skylab 4 84 Days	1D	CDR	522	1419
	2D	SPT	2395	976
	3D	PLT	1040	1283

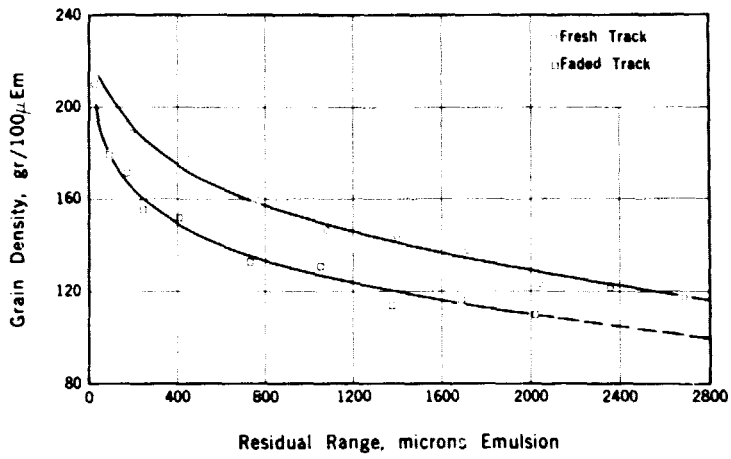


Figure 1
Grain Density of Fresh and Faded Proton Track in Ilford G.5 Emulsion

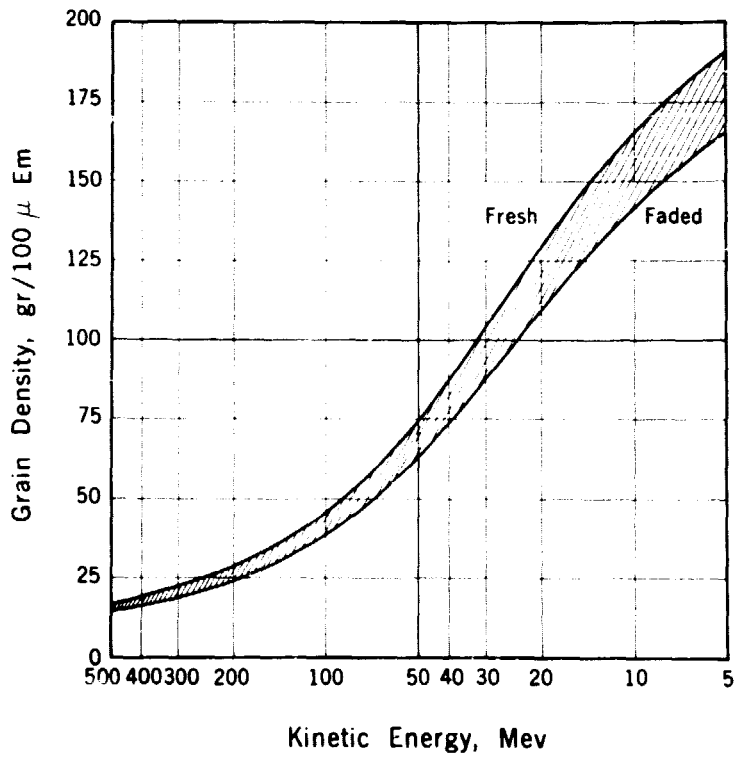


Figure 2
Grain Density/Energy Function for Fresh and Faded Proton Track in Ilford G.5 Emulsion

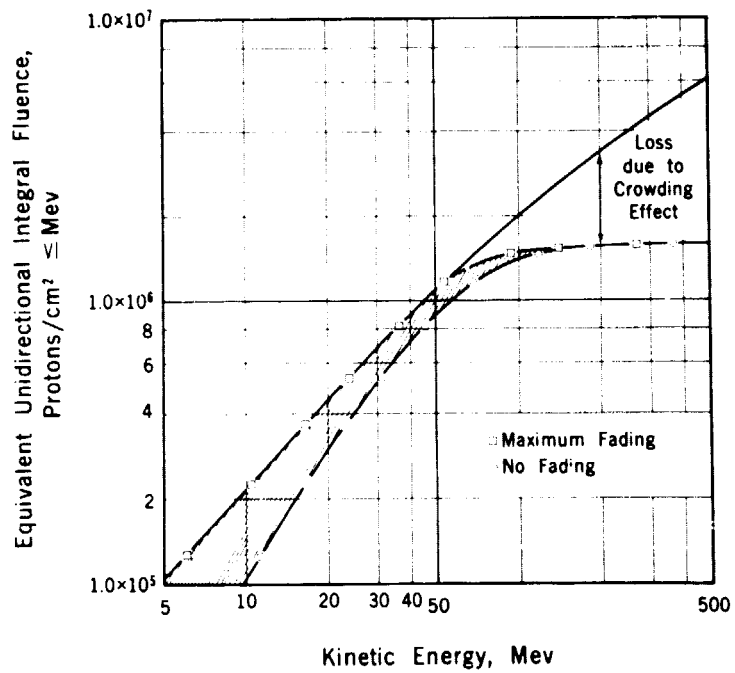


Figure 3

Integral Energy Spectrum of Protons on Skylab 2

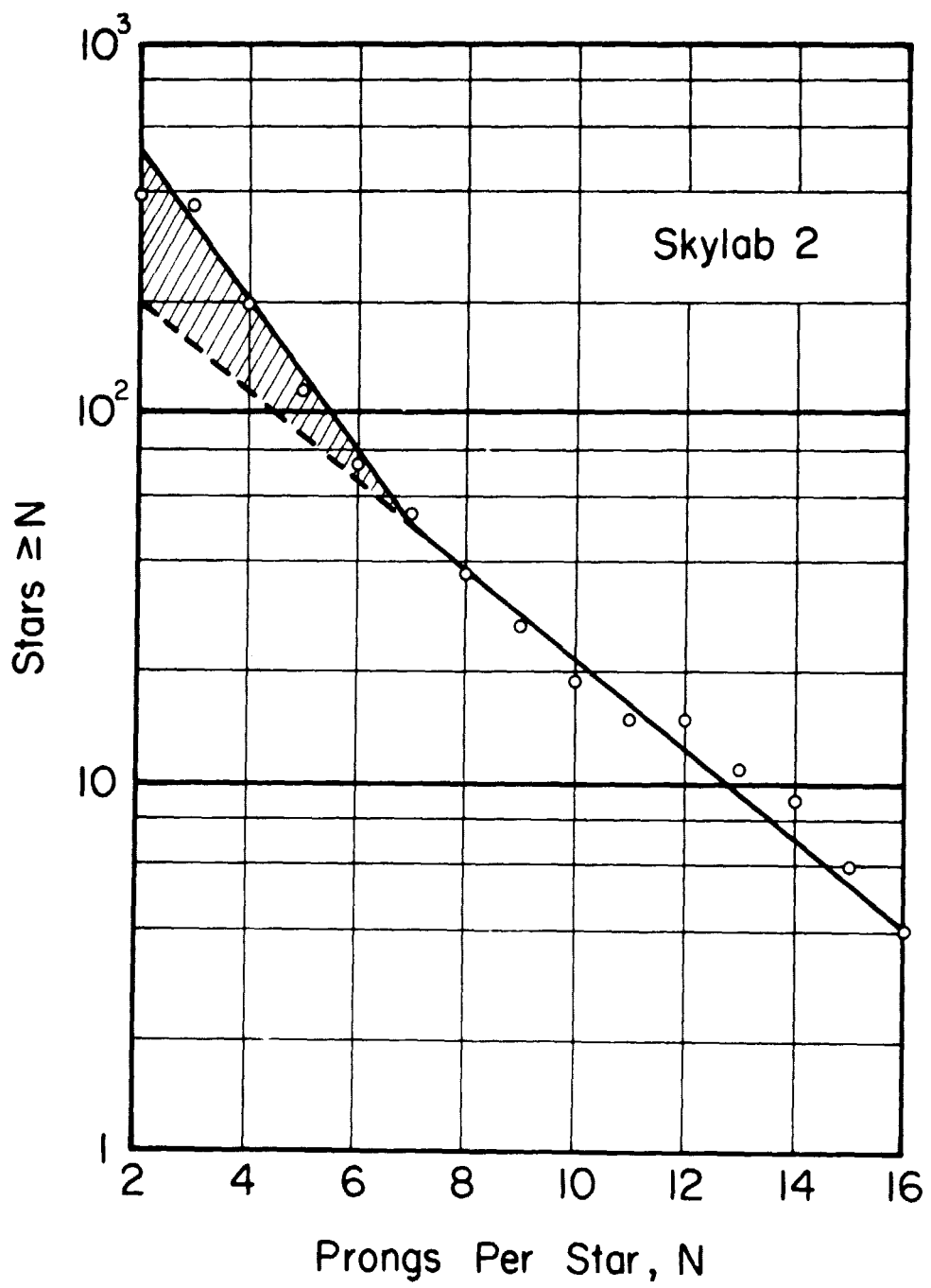


Figure 4

Integral Prong Spectrum of Star Population in Ilford K.2 Emulsion Flown on Skylab 2

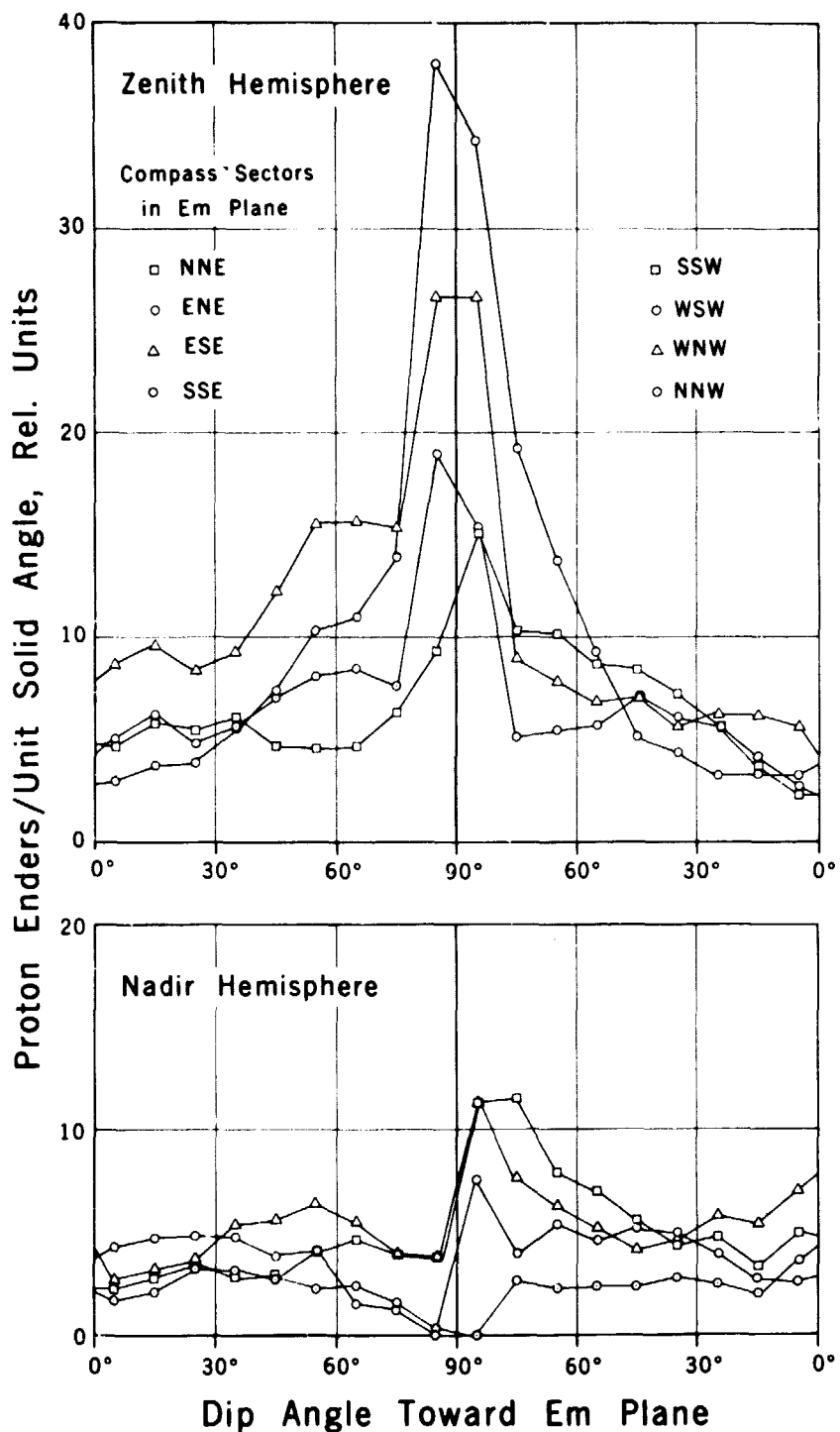


Figure 5

Directional Distribution of Proton Ends in Film Vault Drawer F on Skylab 2